Available on CMS information server

CMS NOTE 2002/017

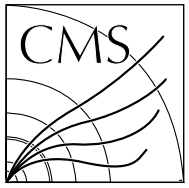

The Compact Muon Solenoid Experiment

CMS Note

Mailing address: CMS CERN, CH-1211 GENEVA 23, Switzerland

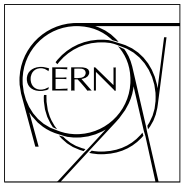

14 June 2002

BEAM TEST RESULTS OF A LONGITUDINALLY SEGMENTED QUARTZ FIBER CALORIMETER WITH HIGH-ENERGY ELECTRONS AND PIONS

N. Akchurin[1)], A. S. Ayan[1)], Gy. L. Bencze[2)], I. Dumanoğlu[3)], E. Eskut[3)], A. Fenyvesi[4)], A. Ferrando[5)], M. C. Fouz[5)], O. Ganel[6)], V. Gavrilov[7)], Y. Gershtein[7)], C. Hajdu[2)], M. I. Josa[5)], A. Kayis-Topaksu[3)], A. Khan[5)], S. B. Kim[8)], V. Kolosov[7,a)], M. Kossov[7)], S. Kuleshov[7)], D. Litvinsev[7)], J.-P. Merlo[1)], J. Molnar[4)], Y. Onel[1)], G. Önengüt[3)], N. Özdeş-Koca[3)], D. Osborne[8)], A. Penzo[9)], A. Polatöz-Kuzucu[3)], J. M. Salicio[5)], V. Stolin[7)], L. Sulak[8)], J. Sullivan[8)], A. Ulyanov[7)], A. Umashev[7)], S. Uzunian[7)], G. Vesztergombi[2)], D. Winn[10)], R. Winsor[1)], P. Zalan[2)], M. Zeyrek[11)]

Abstract

We present the results of test beam studies of a longitudinally segmented quartz fiber calorimeter prototype constructed in the process of developing the CMS forward calorimeter. This particular prototype consists of fully independent electromagnetic and hadronic sections. We discuss equalization of reconstructed energies for electrons and pions and describe in detail the measured performance.

[1)] University of Iowa, Iowa City, U. S. A.

[2)] KFKI-RMKI, Budapest, Hungary.

[3)] Çukurova University, Adana, Turkey.

[4)] ATOMKI, Debrecen, Hungary.

[5)] CIEMAT, Madrid, Spain.

[6)] Texas Tech University, Lubbock, U. S. A.

[7)] ITEP, Moscow, Russia.

[8)] Boston University, Boston, U. S. A.

[9)] Università de Trieste and INFN, Sez. Trieste, Trieste, Italy.

[10)] Fairfield University, Fairfield, U. S. A.

[11)] Middle East Technical University, Ankara, Turkey.

[a)] Corresponding author. E-mail: Victor.Kolosov@itep.ru, Fax: +7-(095)-127-08-33, Phone: +7-(095)-125-9542

1 Introduction

The forward calorimeters in CMS [1, 2] will cover the pseudorapidity range $3 \leq |\eta| \leq 5$. They improve the missing transverse energy resolution and enable the identification of very forward jets. The measurement of E_t^{miss} is essential in top quark production studies, as well as for Standard Model Higgs searches in channels containing neutrinos. In much the same way, the forward calorimeters provide for better hermeticity and are necessary for SUSY particle searches.

The production of Higgs bosons ($m_H \approx 100 - 1000$ GeV) through the WW or ZZ fusion mechanism is characterized by the appearance of two forward *tagging jets* in the pseudorapidity range of $2.0 \leq |\eta| \leq 5.0$. These jets are energetic ($< p > \approx 1$ TeV) and have a transverse momentum of the order of m_W. The detection of these tagging jets by the forward calorimeters aids in reducing the large QCD background against the Higgs signal.

In all these cases, a moderate calorimeter energy resolution and granularity are needed. A good reconstruction of the energy flow and jet energies demands a degree of equalization of hadron and electromagnetic shower signals. Large energy fluctuations between gammas and hadrons in a jet make it imperative to seek a certain equalization in the detector response to electrons and to charged hadrons in order to correctly define the energy scale that the calorimeter measures. The methodology that accomplishes this for single particles is discussed in detail in Section 5 of this paper.

We presented the test beam results of a single quartz calorimeter prototype and discussed the general features of Čerenkov calorimetry in detail in a previous paper [9]. In this paper, we focus on a longitudinally segmented calorimeter consisting of two independent sections, *i.e.* electromagnetic (EM) and hadronic (HAD) sections.

2 Čerenkov Calorimetry

A charged particle traversing a quartz fiber with a velocity greater than the speed of light in quartz, emits Čerenkov radiation. The opening angle of the Čerenkov cone, θ_c, is related to the speed of the particle, β, $\cos\theta_c = 1/n\beta$, where n is the refraction index of the fiber. There is a threshold value ($\beta_{\min} = 1/n$), below which there is no Čerenkov radiation. The light yield, in photons, due to the Čerenkov effect [10, 11], is given by:

$$N_{pe} = L\frac{\alpha^2 z^2}{r_e m_e c^2}\int \epsilon_{coll}(E)\epsilon_{det}(E)\sin^2\Theta_c(E)dE \tag{1}$$

The particles entering the calorimeter absorber make showers of particles. Amongst them, those entering in a quartz fiber with β close to 1 are essentially electrons. The electrons producing light in a quartz fiber are roughly those entering in the fiber with an angle of $\sim 45^\circ \pm 10^\circ$ [5].

The implication is that the apparent shower development in fiber calorimeters is dramatically different from the one observed in dE/dx calorimeters: The showers appear to be very narrow. For electron showers, the transverse development is narrower than the Moliere radius of the absorber. For pions, the apparent radial size is roughly 1/2 an interaction length of the absorber. In both cases, we are referring to 90% energy containment [9].

In a hadronic shower, secondary electron production is directly related with the π^0 and η production in the absorber. Thus the light collection in hadron showers is dominated by the statistical fluctuations in the production of these particles. At very large energies the π^0 fraction is expected to be ~100%, but at $\sqrt{s} = 14$ TeV, the energies of the single charged pions are not very large. The mean value is ~ 8 GeV/particle due to pile-up. Therefore, the response of a Čerenkov calorimeter to a photon will always be higher than that of to a charged pion of the same energy: $e/\pi > 1$.

What is true for single particles also applies to forward jets. For instance, the ones produced in association with a Higgs bosons, have a high multiplicity (~ 30) with a large fluctuation in its gamma content. The average particle energy in a jet is about 70 GeV. Jets that are rich in gammas will give a higher signal than those with a poor gamma fraction for the same jet energy. If it is not properly attended, the calorimeter jet energy reconstruction will suffer because of this effect.

One way of solving the problem is to use a longitudinally segmented calorimeter (two or more sections). With more than one segment, it is possible to weight the signals from each section to make the reconstructed energy equal for electromagnetic and hadronic particles. The reconstruction of jets should also be improved because the energy reconstruction will no longer depend on the fraction of the energy carried by the gammas. The same applies to the total energy flow in the forward direction.

3 Experimental Setup and Test Beam

The calorimeter consists of two independent modules (figure 1). Each module is a copper block with fibers embedded in it in such a way that every fiber is equidistant to its six nearest neighbors with the spacing 2.3 mm. The resulting quartz filling fraction in the volume is 1.5%. The EM section is 34 cm, while the HAD section is 135 cm long. The equivalent lengths for EM and HAD modules are 23 $X_0(2\lambda_I)$ and 8.5 λ_I respectively. Thus the total length is about 10.5 λ_I. The instrumented volume is sufficient for 93% lateral and full longitudinal hadron shower containment[9].

The fibers are arranged to form 9 readout towers with $53 \times 54\ \mathrm{mm}^2$ transverse dimensions. The Čerenkov light originated in the fibers of each tower is detected by the photomultiplier (PMT) and digitized. The PMTs of the EM section are mounted in front of the module to avoid a gap between the EM and HAD sections (see figure 1). Čerenkov light, mostly going in the forward direction along the fibers, is collected in the EM section by means of reflection at the mirrored ends of the fibers. This design was later changed where all fibers are readout from the back and longitudinal segmentation is accomplished by the use of different length fibers [2].

The calorimeter was mounted on a movable platform in the H4 beam line of the CERN SPS. The platform could be moved vertically and horizontally in the plane transverse to the beam line so that the center of each tower could be moved into the beam as needed. The angles between the beam and the fibers both in horizontal and vertical planes were kept at 0° throughout the experiment. The details of the beam line rates, the trigger conditions, and the readout system can be found in [9].

4 Data Analyses

The data sample used for the analysis consists of

1. electron data at 10, 12, 15, 20, 35, 80, 100, 150, 200 GeV,
2. negative pion data at 35, 80, 100, 200, 300, 350 GeV, and
3. calibration data that were taken with 80 GeV electrons with the beam centered on individual towers of both the electromagnetic and hadronic modules.

For both sections, the gains were set at approximately 500 ADC counts above the pedestal value for 80 GeV electrons. The calibrated responses of all cells to 80 GeV electrons were equalized using individual factors for each channel. The calibration coefficients for every tower were calculated assuming that all of the electron beam energy was contained in a given tower. These factors defined the electromagnetic scale for the prototype signal.

5 Results for Single Particles

The response of the calorimeter to both pions and electrons was calculated as a sum of signals from 18 towers (3×3 towers). Figures 2 and 3 illustrate the response function to 200 GeV electrons and pions, respectively. Electron showers are almost fully contained in the EM section, but the pion signal is shared between EM and HAD sections as illustrated in figure 4. In addition, the response function for 200 GeV pions for the HAD section alone was compared with the distribution for HAD section when the deposited energy in EM section was less than 3 GeV (see figure 5).

The mean values and RMS of the signal for pions and electrons are listed in Tables 1 and 2. The mean value of the response as a function of the particle energy is shown in Fig.6. In the measured energy range, both electrons (full circles) and pions (full triangles) show a linear dependence. Empty circles and triangles in Fig. 6 correspond to the GEANTsimulation expectations [12] and show good agreement with data. The measured energy resolutions for electrons and pions are given in Figs. 7 and 8, respectively. The curves correspond to fits of form:

$$\begin{array}{ll} \sigma_{RMS}/E = (1.5 \pm 0.01)/\sqrt{E} \oplus (0.06 \pm 0.002), & \text{for electrons} \\ \sigma_{RMS}/E = (2.7 \pm 0.02)/\sqrt{E} \oplus (0.13 \pm 0.002), & \text{for pions.} \end{array} \tag{2}$$

These results are in full agreement with the measurements using a non-segmented prototype [9] except for the constant term in the electron energy resolution. The value given in [9] is < 0.02. The higher value found in the present data is most probably due to non-uniformities in the reflection efficiency of the mirrored ends of the fibers

of the EM module. Empty circles in Figs. 7 and 8 correspond to the GEANTexpectations. The simulated and measured values have, within the errors, the same stochastic coefficients, the same apply for the constant term for electrons. In the case of pions, the constant term found in the simulation is by 10–20% smaller than in the data. It means that the fluctuations of the electromagnetic component of the hadronic showers in copper are underestimated by GHEISHA[12]. GHEISHAwas chosen to simulate the response of the quartz fiber calorimeter because it gave more realistic e/π-ratio behaviour.

As seen in Fig. 6, the response for pions is much lower than that of electrons at any energy. This is a consequence of the Čerenkov mode of operation, that implies $e/\pi > 1$. However, with a longitudinally segmented calorimeter, one can weight the observed signals in each of the modules in an attempt to equalize the reconstructed energies for electrons and pions. The real equalization can be achieved only at the energy where the mean response for pions and electrons is equal, due to significant energy non-linearity for pions. This is done by writing the reconstructed energy as:

$$A = C_1 A_{EM} + C_2 A_{HAD} \tag{3}$$

For a wide energy range, for each value of the ratio C_2/C_1, the coefficients C_1 and C_2 can be recalibrated to provide the correct energy reconstruction in terms of the mean value of the amplitude for all energy points. These coefficients can be found using the following equation:

$$\sum < (A - E) >= 0 \tag{4}$$

where the sum extends to electrons and pions at all energies.

Equalizing the mean signal for electrons and pions at 100 GeV we find:

$$C_2/C_1 = 1.97. \tag{5}$$

For this value, the reconstructed energy, as a function of the beam energy is shown in Fig. 9. The dotted line represents $A/E = 1$. As is well known, the introduction of two calibration constants for the reconstruction of the energy degrades the hadronic energy resolution. In this case:

$$\sigma/E = 2.9/\sqrt{E} \oplus 0.2 \tag{6}$$

The electron energy resolution remains unchanged since the electron showers are almost fully contained in the EM section.

6 Summary and Conclusions

The fast signal speed, narrow lateral profile and low sensitivity to neutrons and radioactive decays allow for better separation of jets from background with respect to other calorimetric techniques. One of the purposes of the CMS forward calorimeters will be the detection and energy measurement of tagging jets. The non-compensating feature of the quartz fiber calorimeter, however, puts some limitations on the jet energy resolution because the fraction of the energy carried by gammas strongly fluctuates. The longitudinal segmentation of the calorimeter allows approximate equalization of the signals from gammas and charged pions of the same energy.

A calorimeter prototype consisting of two independent modules, each made of a block of copper with embedded quartz fibers, was tested using electrons and pions at the CERN SPS H4 facility. The prototype is 10.5 interaction lengths deep. By using two calibration constants in energy reconstruction, from the signals measured in each of the sections, we can reach a level of equalization of the reconstructed energy for electrons and pions. For single particles, the measured energy resolutions in the prototype are:

$$\begin{array}{ll} \sigma_{RMS}/E = (1.5 \pm 0.01)/\sqrt{E} \oplus (0.06 \pm 0.002), & \text{for electrons} \\ \sigma_{RMS}/E = (2.7 \pm 0.02)/\sqrt{E} \oplus (0.13 \pm 0.002), & \text{for pions.} \end{array} \tag{7}$$

Although it allows a correct reconstruction of the energy, this two-segment solution has a drawback in that there will be appreciable noise in the EM fiber bundles facing the interaction point. Other approaches for obtaining a direct equalization of the electromagnetic and hadronic signals are based on the partial suppression of the electromagnetic signal. This can be achieved by the use of fibers of different length [2] inside the absorber. The latter geometry is what is adopted for the CMS forward calorimeters.

7 Acknowledgments

We would like to thank our colleagues from CMS, and in particular J.Bourotte and M.Haguenauer, who made the described beam tests possible. We are grateful to N.Doble, who provided us with particle beams of excellent quality. This project was carried out with financial support from CERN, the U.S. Department of Energy, National Science Foundation (NSF-INT-98-20258), RMKI-KFKI (Hungary, OTKA grant T 016823), the Scientific and Technical Research Council of Turkey (TÜBITAK), CICYT (Spain, grant AEN96-2051-E), the International Science Foundation (grants M82000 and M82300), the State Committee of the Russian Federation for Science and Technologies, and the Russian Research Foundation (grant 95-02-04815), CERN-INTAS grant 99-0377.

References

[1] The CMS Collaboration. Technical Proposal. CERN/LHCC 94-39, 1994.

[2] The CMS Collaboration, *The Hadron Calorimeter Project Technical Design Report*, CERN/LHCC 97-31 (1997)

[3] A. Contin *et al*, *R&D Proposal for Development of Quartz Fibre Calorimetry*, CERN DRDC/94-4 (1994)

[4] G. Anzivino *et al*, Nucl. Instr. and Meth A 357 (1995) 380.

[5] P. Gorodetzky *et al*, Nucl. Instr. and Meth A 361 (1995) 1.

[6] A. Ferrando *et al*, Nucl. Instr. and Meth B 83 (1993) 205.

[7] V. Gavrilov *et al*, CMS TN-94-324.

[8] P. Gorodetzky *et al*, Nucl. Instr. and Meth. A 361 (1995) 161-179

[9] N. Akchurin *et al*, NIM A 399 (1997) 202.

[10] J. V. Jelly, *Cherenkov Radiation and its Application*, Pergamon Press, 1958.

[11] The European Physical Journal *Particles and Fields*, C 15, 176, 2000.

[12] GEANT Description and Simulation Tool, CERN Program Library Long Write Up W5013.

[13] N. Akchurin *et al*, NIM A 400 (1997) 267-278.

Table 1: The electron response of the prototype and its energy resolution are shown below.

Energy(GeV)	Response(GeV_{EM})	RMS/R
8	8.09 ± 0.05	0.55 ± 0.01
10	9.99 ± 0.05	0.50 ± 0.01
12	12.16 ± 0.05	0.46 ± 0.01
15	15.16 ± 0.06	0.40 ± 0.01
20	19.74 ± 0.06	0.356 ± 0.004
35	34.67 ± 0.08	0.267 ± 0.002
80	77.79 ± 0.12	0.182 ± 0.001
100	100.9 ± 0.1	0.165 ± 0.001
150	153.0 ± 0.2	0.140 ± 0.001
200	191.3 ± 0.2	0.127 ± 0.001

Table 2: The pion response of the prototype and its energy resolution are shown below .

Energy(GeV)	Response(GeV_{EM})	RMS/R
35	19.44 ± 0.11	0.464 ± 0.005
80	47.71 ± 0.17	0.328 ± 0.003
100	63.01 ± 0.18	0.304 ± 0.002
200	130.2 ± 0.3	0.229 ± 0.002
300	202.3 ± 0.5	0.206 ± 0.002
350	237.7 ± 0.4	0.194 ± 0.001

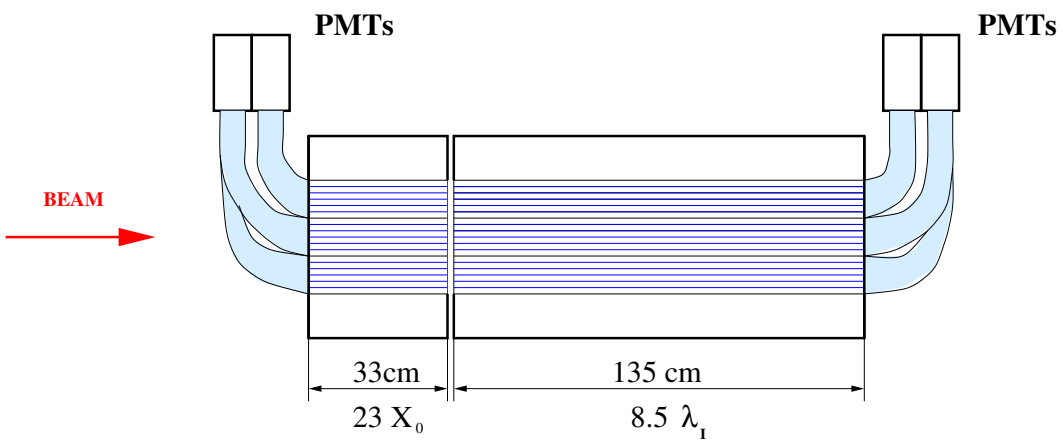

Figure 1: The longitudinally segmented calorimeter consists of two sections: The electromagnetic section (EM) is located upstream of the hadronic section (HAD). The light generated in the EM section travels mostly forward and gets reflected by the mirrors at the fiber ends. In the case of the HAD section, the forward travelling light is detected by the PMTs.

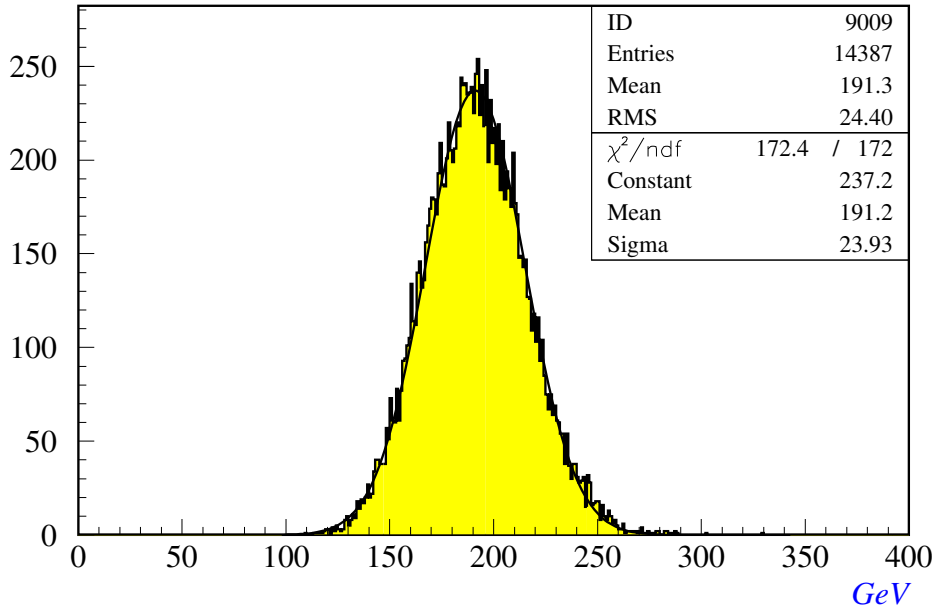

Figure 2: The signal amplitude distribution for 200 GeV electrons is shown above.

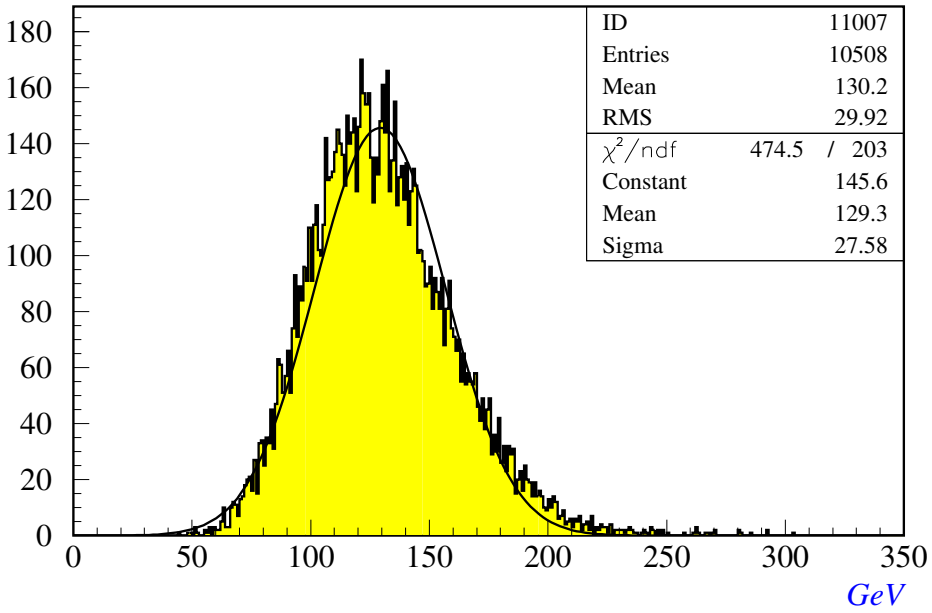

Figure 3: The signal amplitude distribution for 200 GeV pions is shown above.

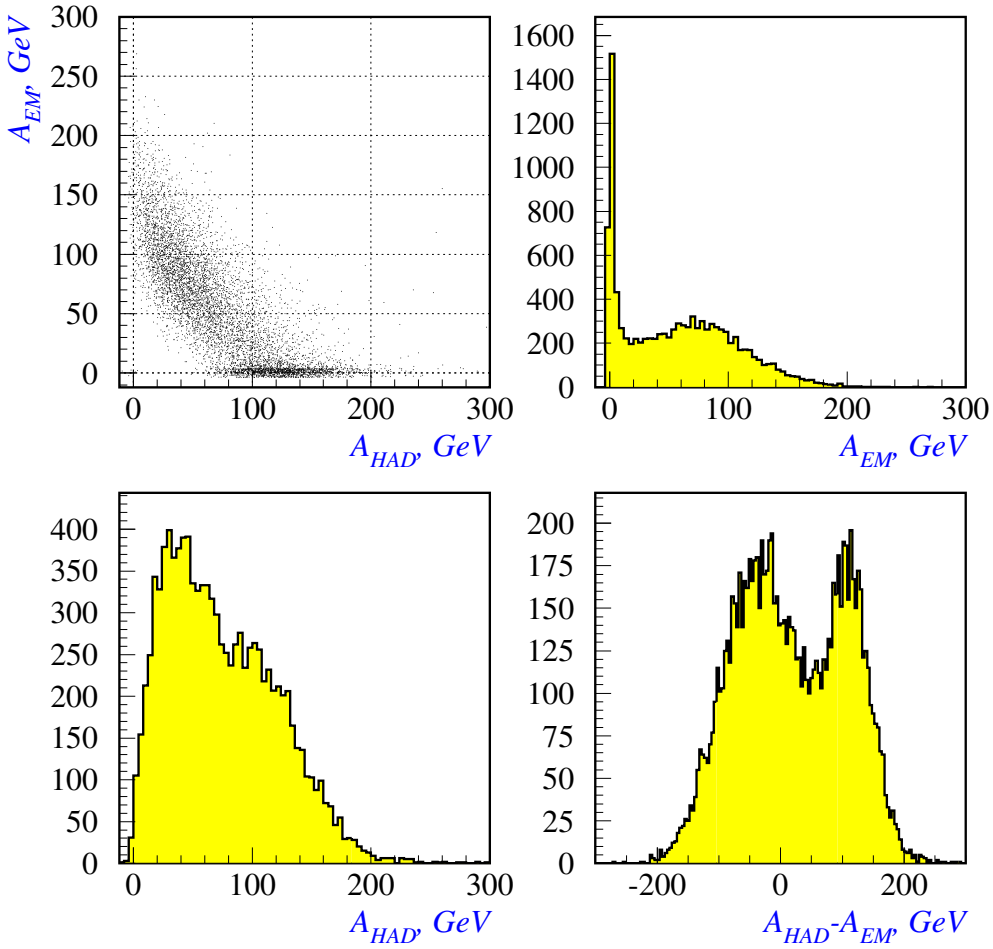

Figure 4: The division of signal between the EM and HAD sections for 200 GeV pions is shown above.

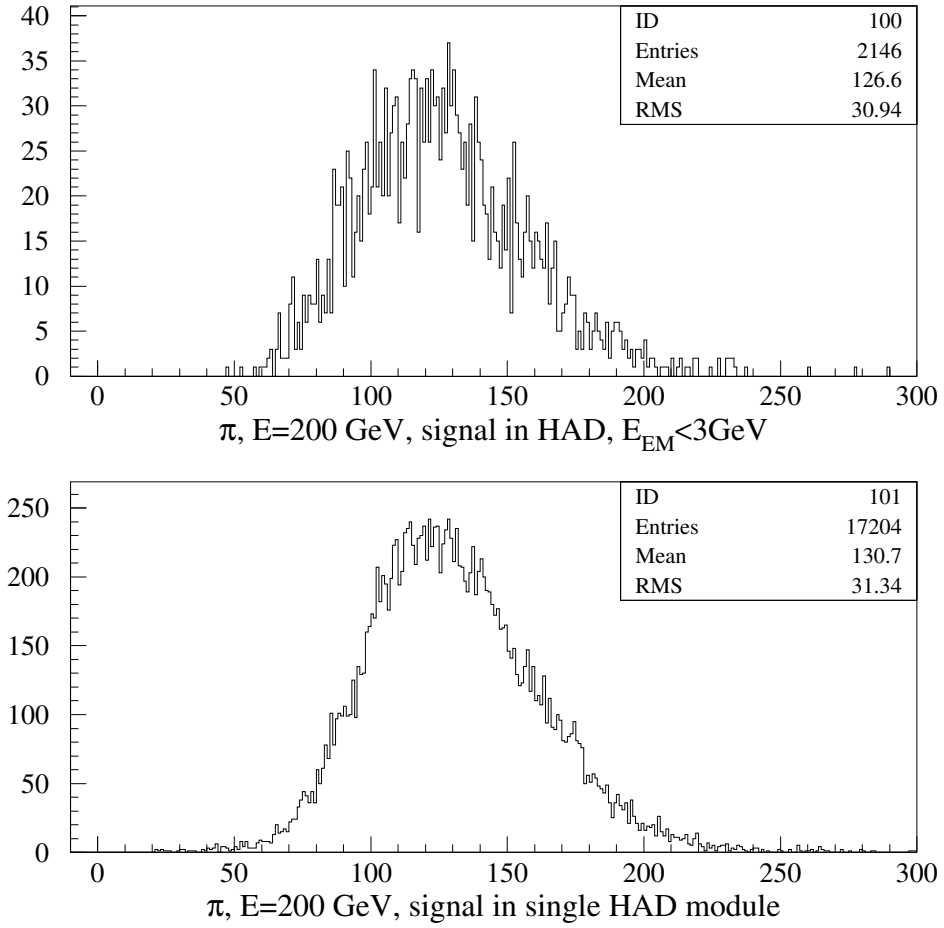

Figure 5: The signal distribution for 200 GeV pions for HAD section is shown (top) when the energy deposition in the EM section is required to be less than 3 GeV. When compared with the signal from the HAD section alone (bottom), there is no significant difference between the two cases.

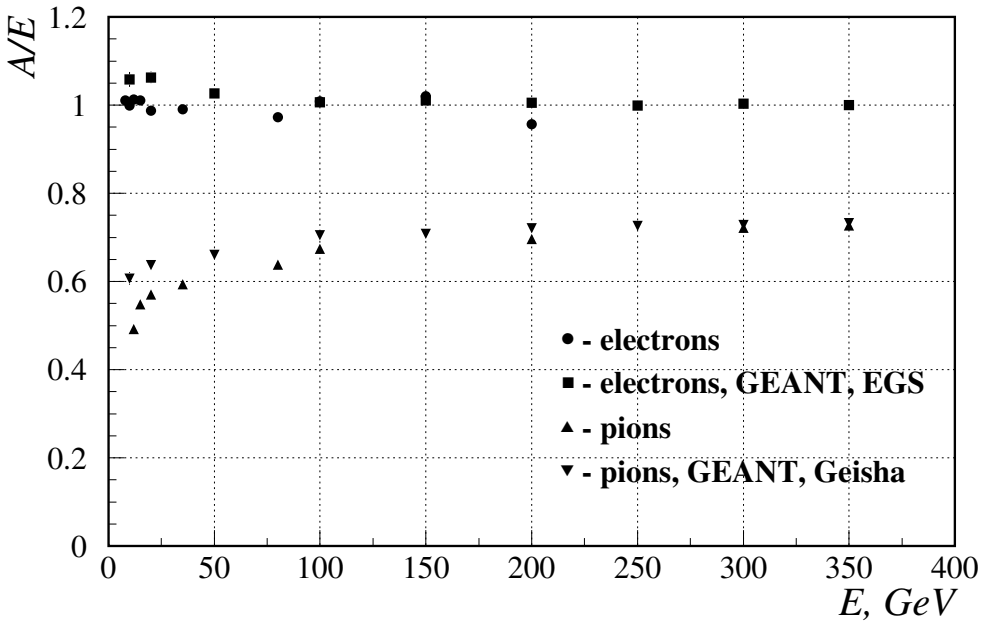

Figure 6: Mean amplitude of signal in the prototype versus energy for electrons and pions for $C_2/C_1 = 1.00$ in comparison with MC results.

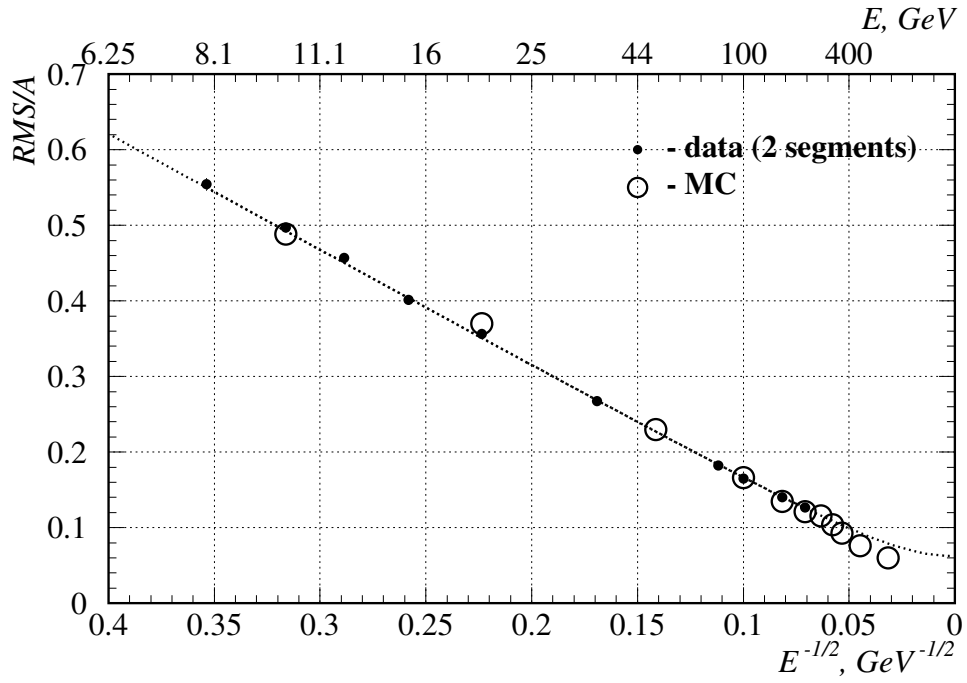

Figure 7: Energy resolution for electrons results in $(1.5 \pm 0.01)/\sqrt{E} \oplus (0.06 \pm 0.002)$.

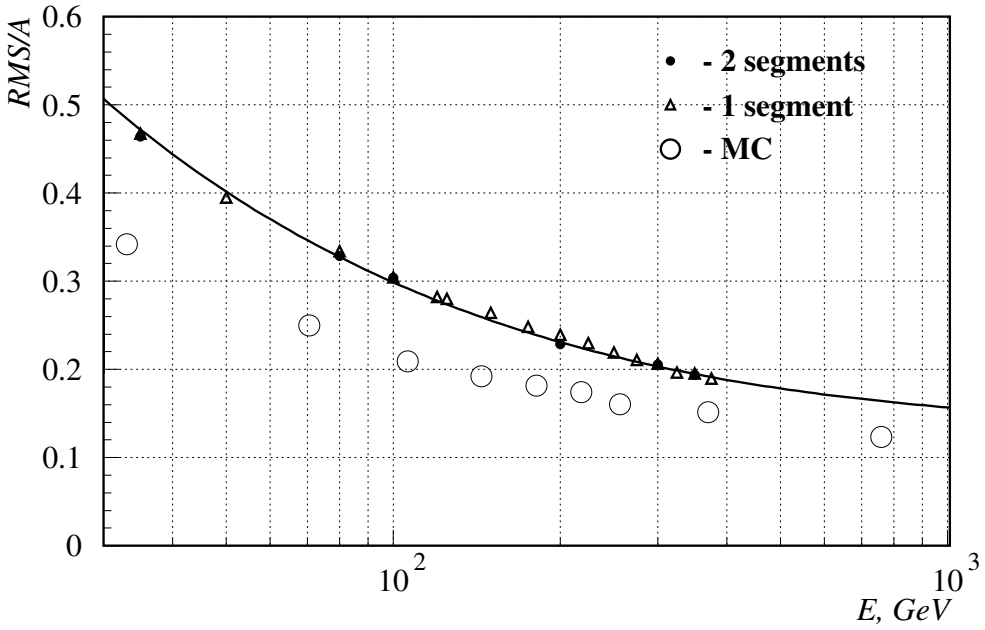

Figure 8: Energy resolution for pions versus energy $1/\sqrt{E}$

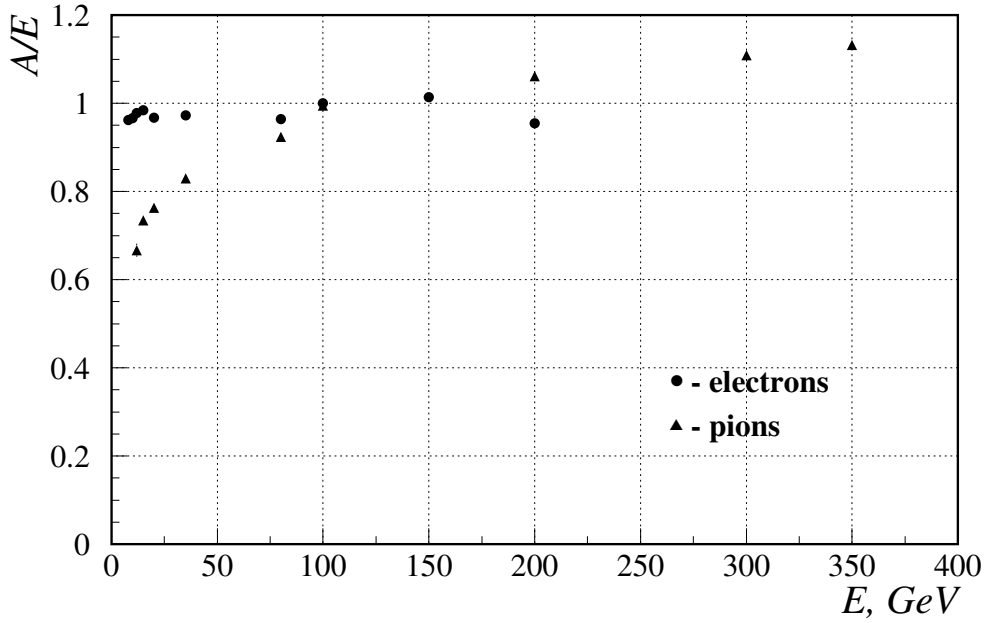

Figure 9: Mean amplitude of signal in the prototype versus energy for electrons and pions for $C_2/C_1 = 1.97$